

# Electric resistivity tomography inversion guided by passive microtremor data for the detection of karst cavities

Daopu Wang\* Dikun Yang<sup>1</sup> Zhentao Yang<sup>1</sup> Qingguo Feng<sup>1</sup> Guihua Long<sup>2</sup> Qingcheng Wang<sup>3</sup>

- 1. Southern University of Science and Technology, Shenzhen, Guangdong, China*
- 2. Shenzhen Municipal Engineering Corp, Shenzhen, Guangdong, China*
- 3. Shenzhen Tagen Group Co.,LTD, Shenzhen, Guangdong, China*

2023.08.29



Gravity, Electrical, Magnetic  
and Electromagnetic  
Research at SUSTech



地球与空间科学系  
DEPARTMENT OF EARTH AND SPACE SCIENCES



南方科技大学  
SOUTHERN UNIVERSITY OF SCIENCE AND TECHNOLOGY



# Outline

**01** | Introduction

**02** | Surveys

**03** | Methods

**04** | Results

**05** | Conclusions

# Biography



## Education

**Southern University of Science and Technology**

**Shenzhen, China**

*Master of Science in Earth and Space Science*

*Sep. 2022 - Jun. 2025 (expect)*

**GPA : 3.56/4.0**

**Yangtze University**

**Wuhan, China**

*Bachelor of Geophysics*

*Sep. 2018 - Jun. 2022*

**GPA : 3.73/5.0**

## Honors & Awards

**2023 3st Prize**, Geophysical knowledge competition for university student

**Hefei, China**

**2021 2st Prize**, Geophysical knowledge competition for university student

**Hefei, China**

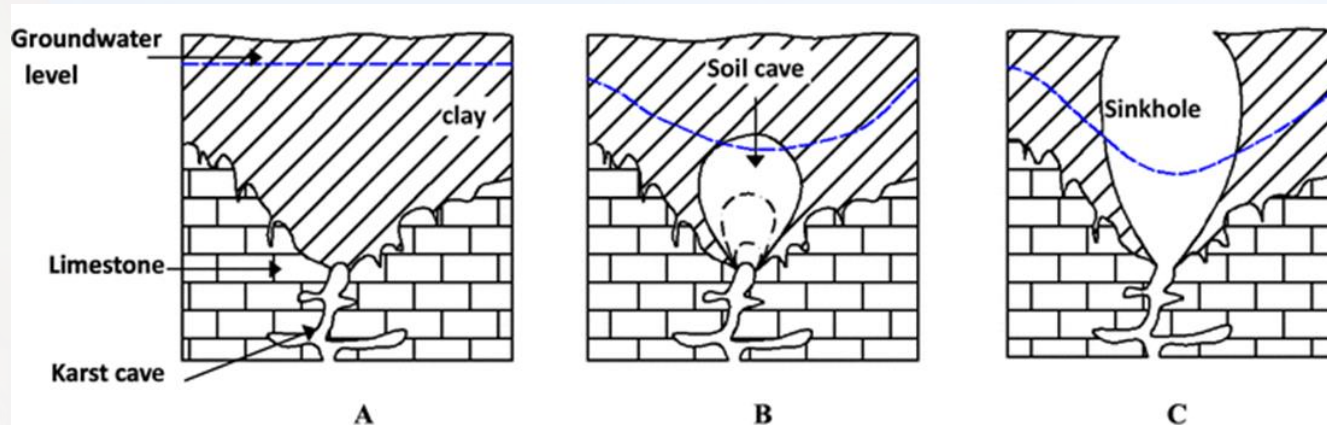
**2019 Winner**, National Inspiration performances

**Hefei, China**

## Specialty

Urban **Near-Surface Geophysical** exploration.





Pipelines , Groundwater extraction...

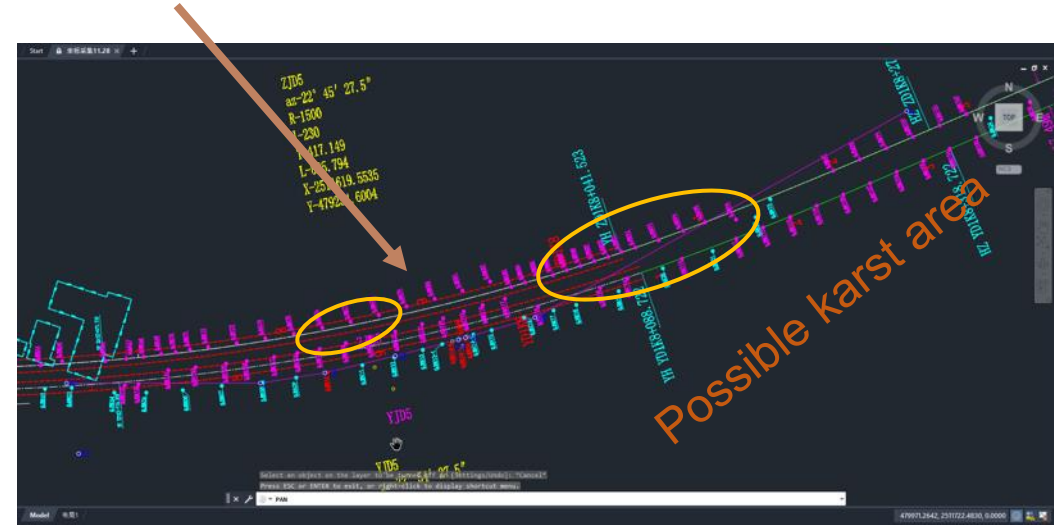
Calcite , Dolomite...





## Pingshan-Dapeng Line (Shenzhen, China)

### Metro tunnels



( Pingshan Station section)

### Karst cavity hazard in Pingshan

Burial depth 10.9 - 73.2 m

Cavity height 0.4 - 21.4 m

Cavity filling Clay, Gravel soil



## ERT (electric)



GD-20

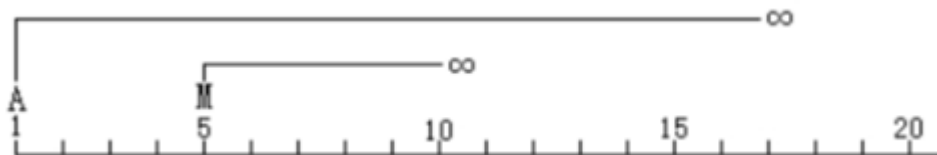


## ANT (passive seismic)



## Pole – Pole

- 40 electrodes
- 5-m spacing



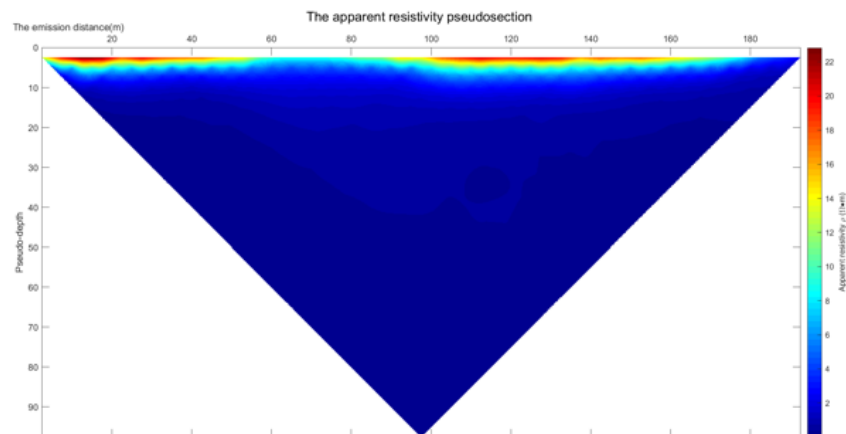
## SmartSolo 16HR 3C

Sample rate : 100Hz

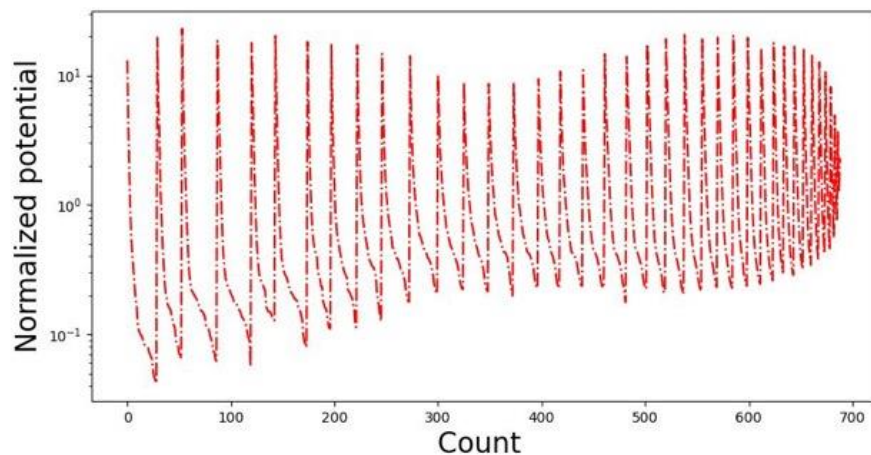
Number of stations : 84

Station distance : 2.5 m

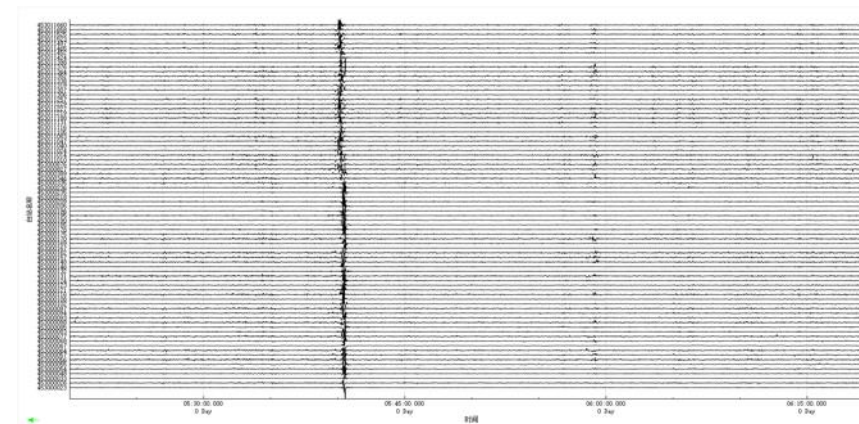
Acquisition time : 30min



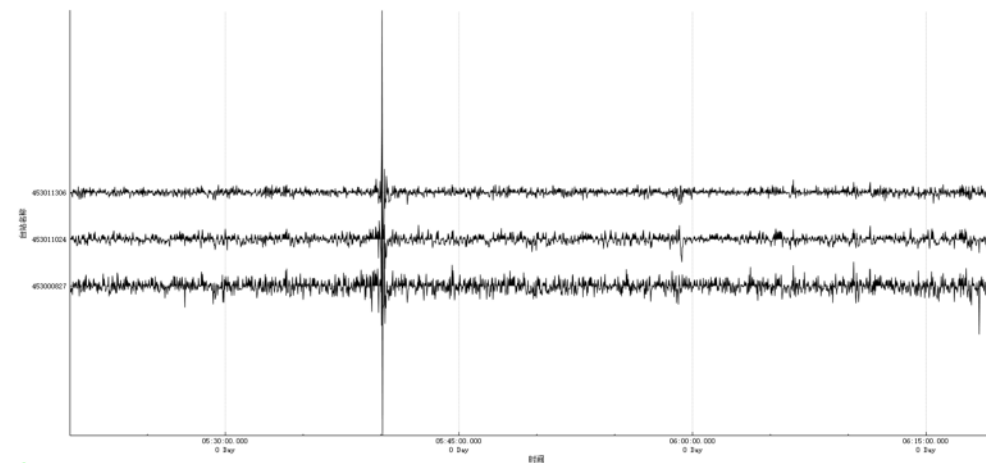
Apparent resistivity pseudo-section



Observed potential difference data plot



Original seismic signals



Passive seismic waveforms

$$\varphi(\mathbf{m}) = \|\mathbf{W}_d(\mathbf{d}_{obs} - \mathbf{f}(\mathbf{m}))\|^2 + \gamma \|\mathbf{W}_m(\mathbf{m} - \mathbf{m}_0)\|^2$$

$$\mathbf{W}_m = (\alpha_s \mathbf{I}, \alpha_x \mathbf{W}_x^T, \alpha_z \mathbf{W}_z^T)^T$$

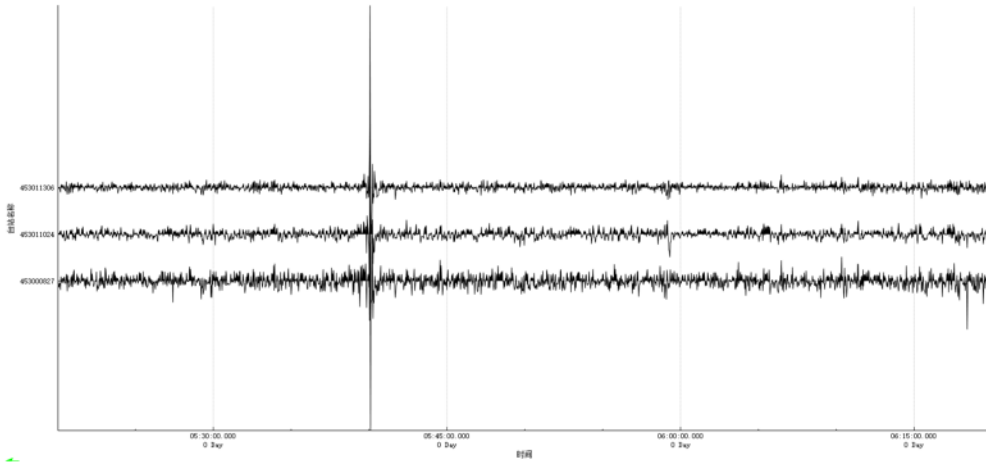
$\mathbf{W}_m$  *model weighting matrix*

$\alpha_s, \alpha_x, \alpha_z$  *Weighting coefficients*

$\mathbf{m}_0$  *Reference and initial model*







## Passive seismic waveforms

- HVSR

The prominent resonant frequency in the H/V spectrum is used to obtain the thickness of the sediment

$$\text{HVSR} = \frac{H(\omega)}{V(\omega)} \quad h = a f_*^b$$

$f_*$  resonance frequency  
 $h$  soil layer thickness

- Extract the dispersion curves

$$I(w, k) = \int_0^{+\infty} C(r, \omega) J_0(kr) r dr \quad \textbf{F-J Method}$$

(Wang et al., 2019)

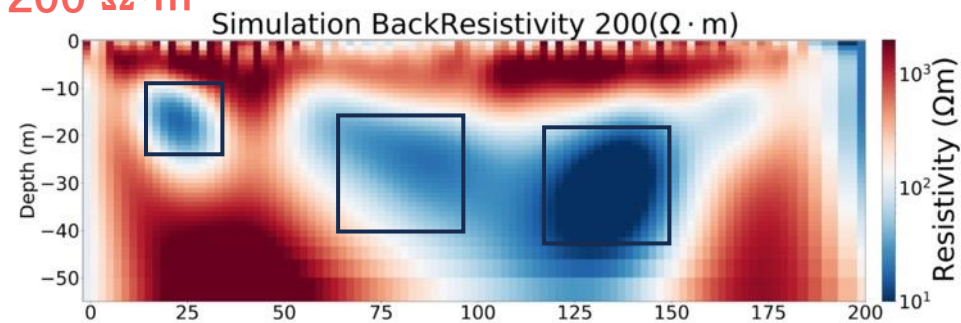
$C(r, \omega)$  Cross-correlation function in frequency  
 $J_0(kr)$  Bessel function

- S-wave velocity

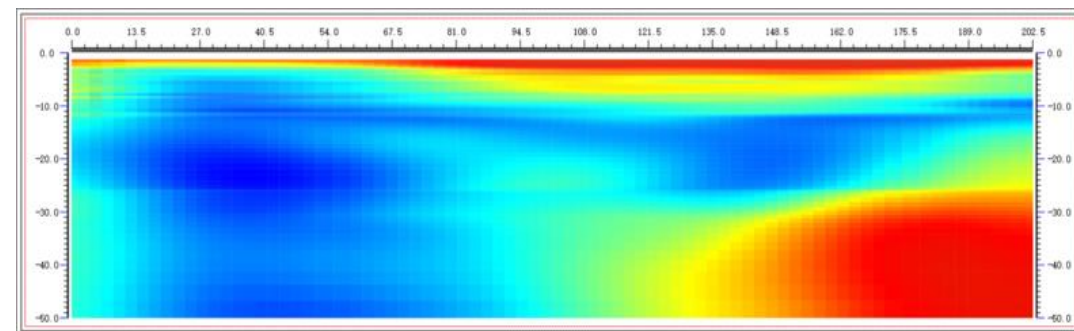
$$f(V_s) = \sum_i \sum_j \text{weight}_j (c_{ij}^s - c_{ij}(V_s))^2$$

(Chen et al., 2019)

$i$  Frequency  
 $j$  Order of the dispersion curve  
 $c_{ij}^s$  Measured phase velocity  
 $c_{ij}$  Theoretical phase velocity

200  $\Omega \cdot m$ 

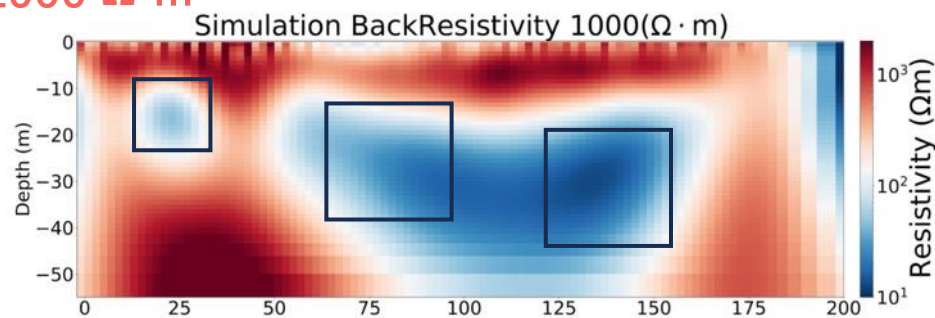
Electrical/seismic structure



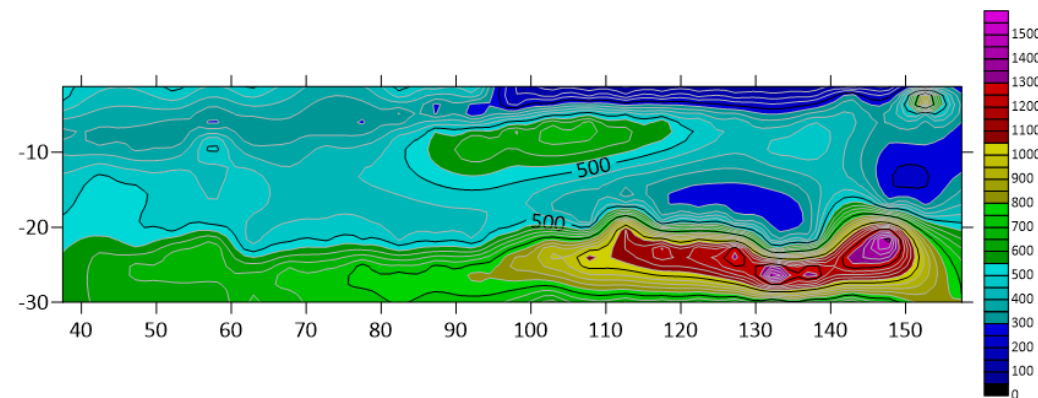
Normalized HVSR image

1000  $\Omega \cdot m$ 

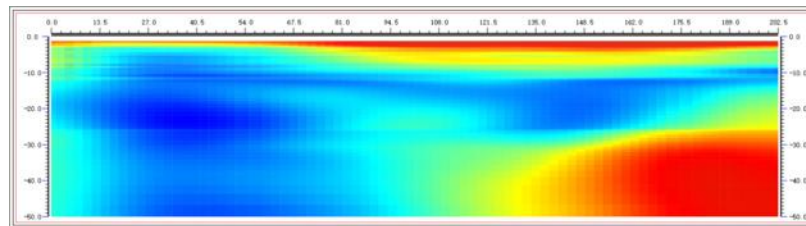
Not consistent



Resistivity Results



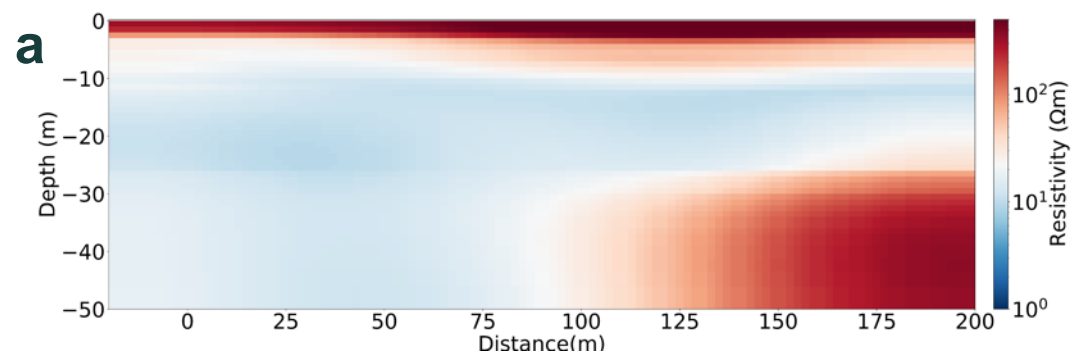
Shear wave velocity image



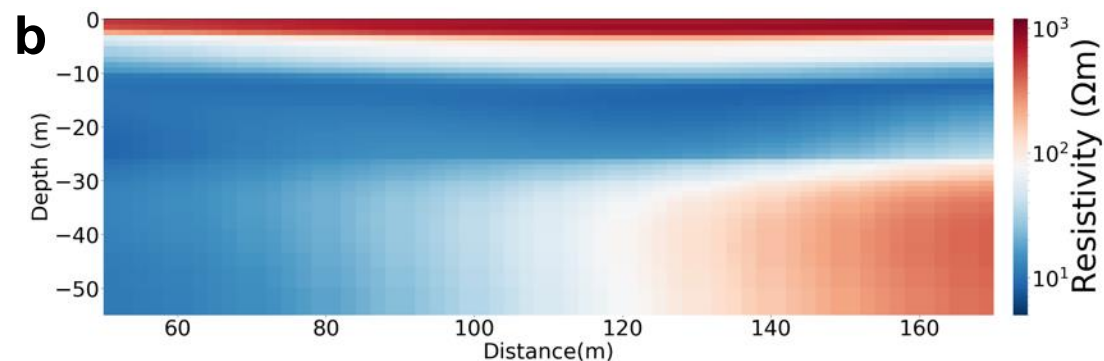
HVSR

Mapping resistivity

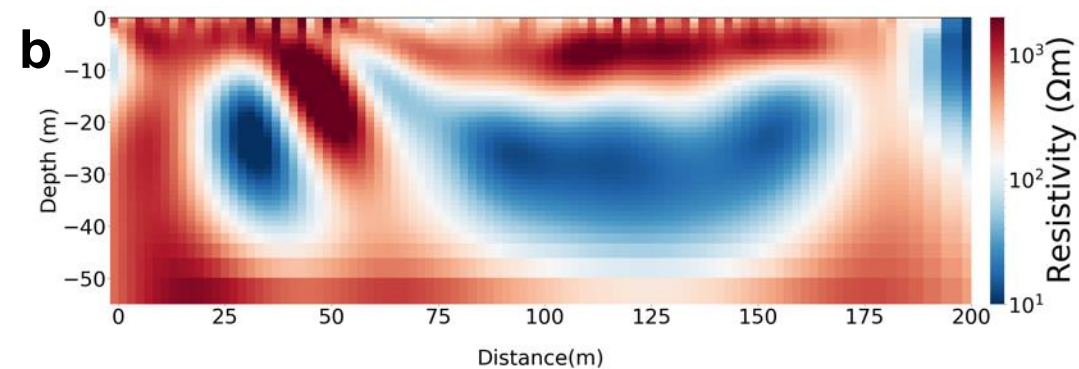
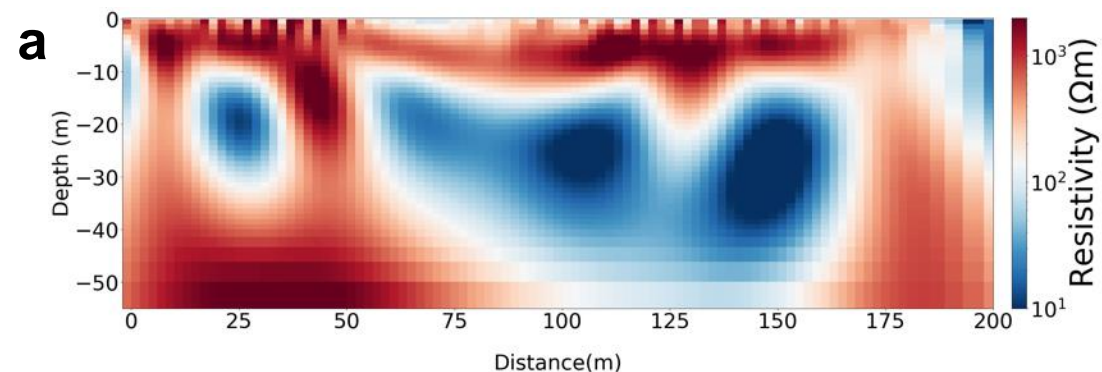
Inverted results



$$\rho = 10^{3 \cdot HVSR}$$

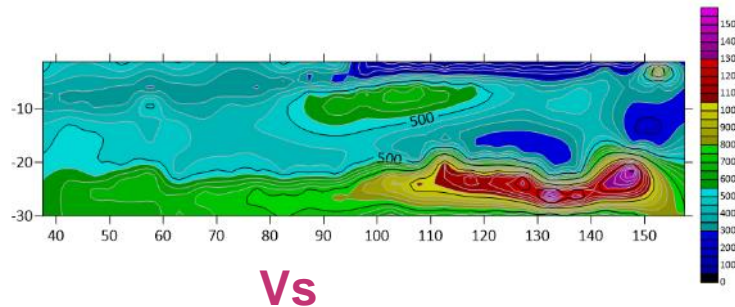
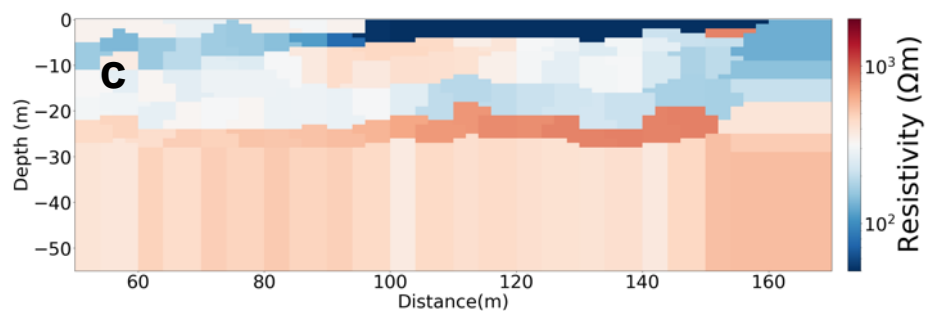
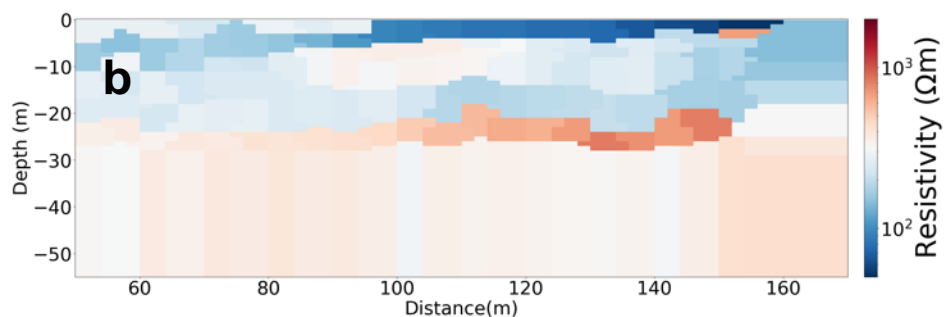
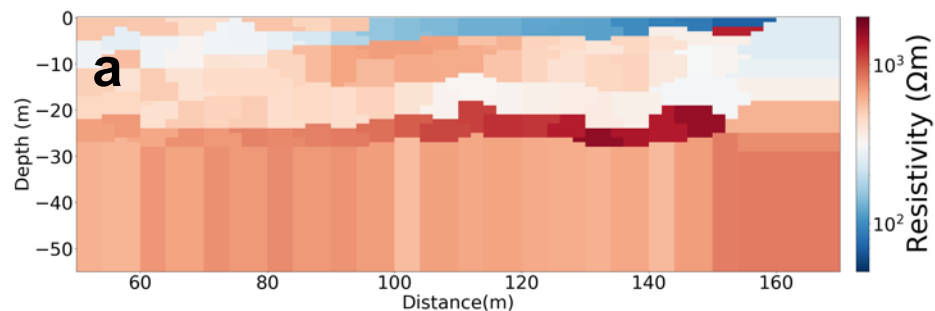


$$\rho = 0.0449(1 + HVSR)^{7.049}$$





## Mapping resistivity

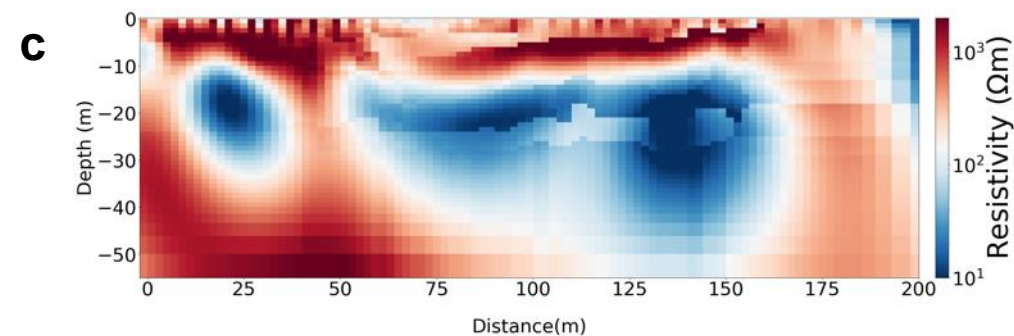
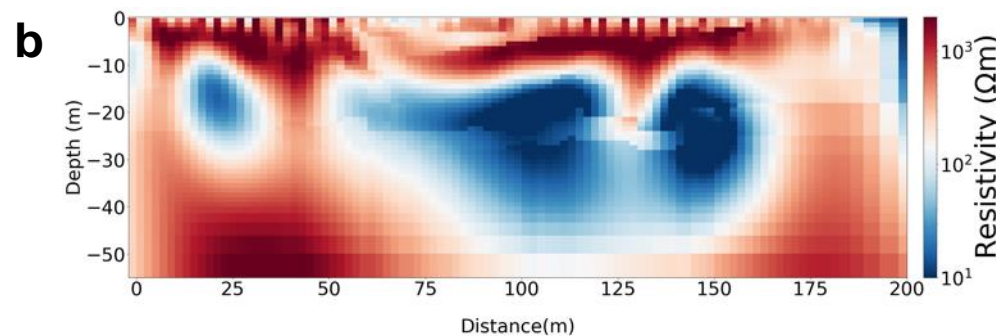
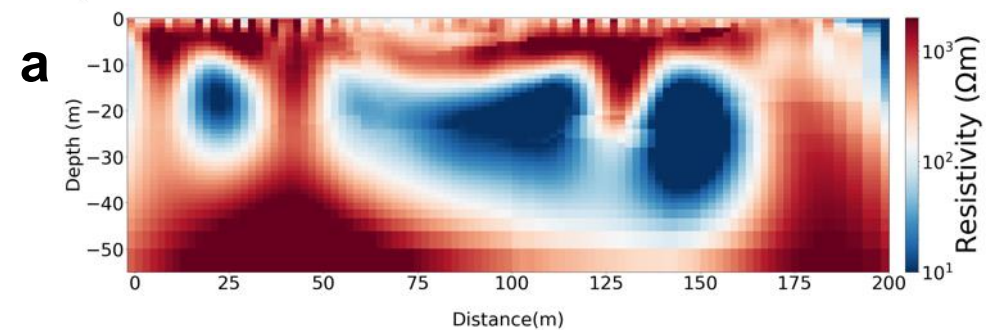


$$\rho = V_s$$

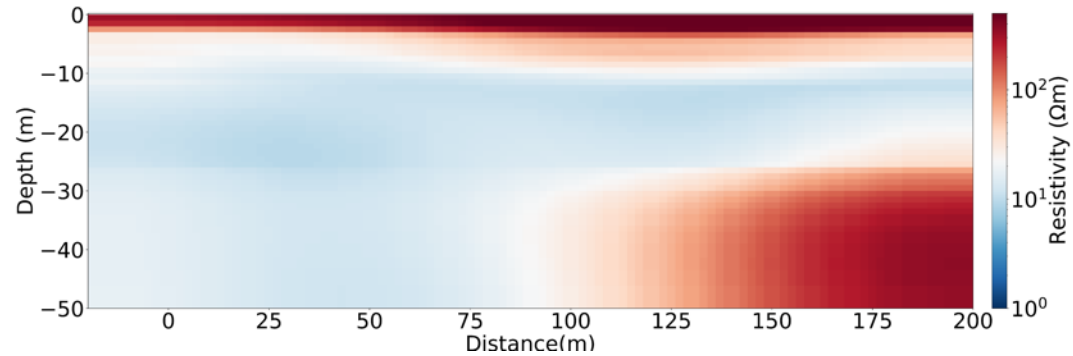
$$\rho = \frac{V_s + 33.289}{1.995}$$

$$\rho = -1.9e-07 * V_s^3 + 1.7e-04 * V_s^2 + 7.39e-01 * V_s - 65.6$$

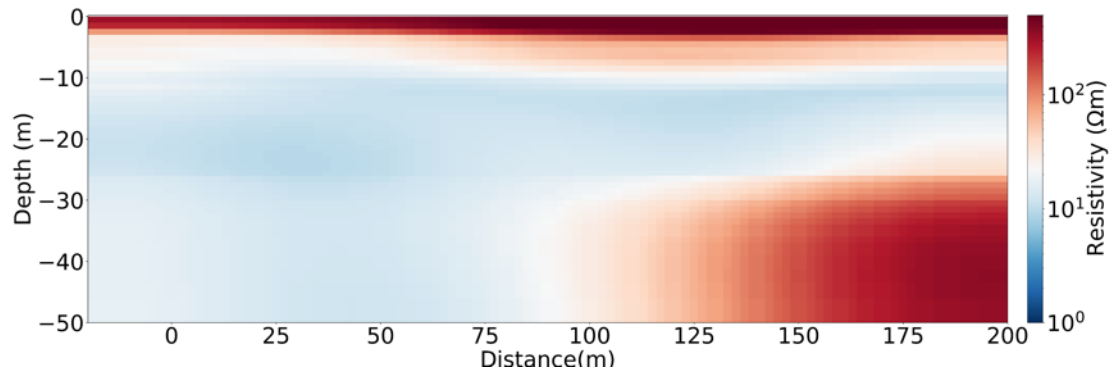
## Inverted results



$$W_m = (\alpha_s I, \alpha_x W_x^T, \alpha_z W_z^T)^T$$



( Initial model )



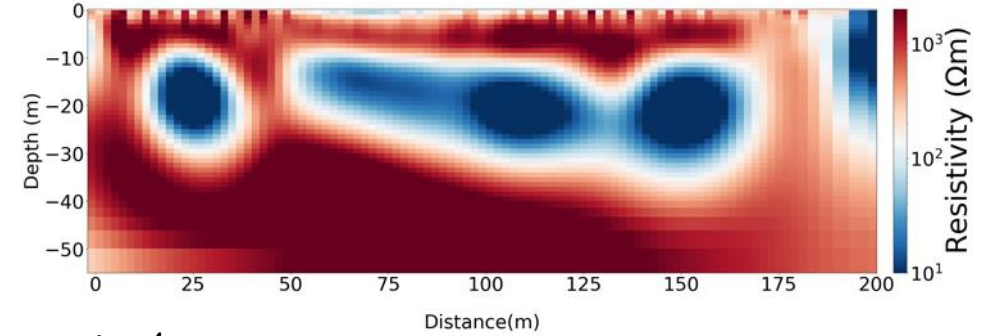
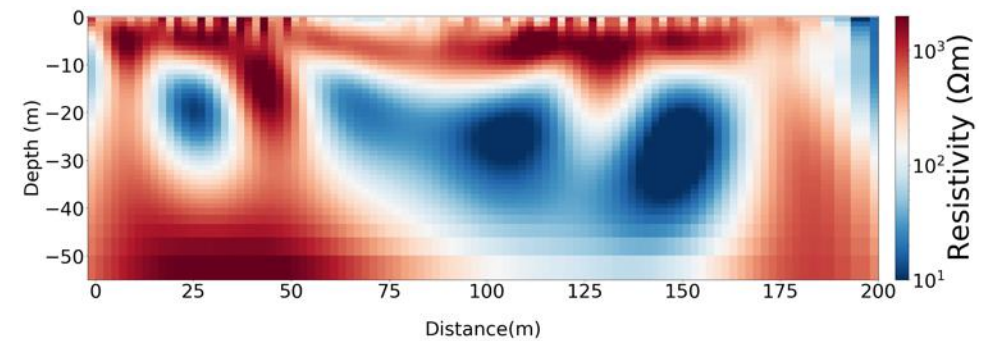
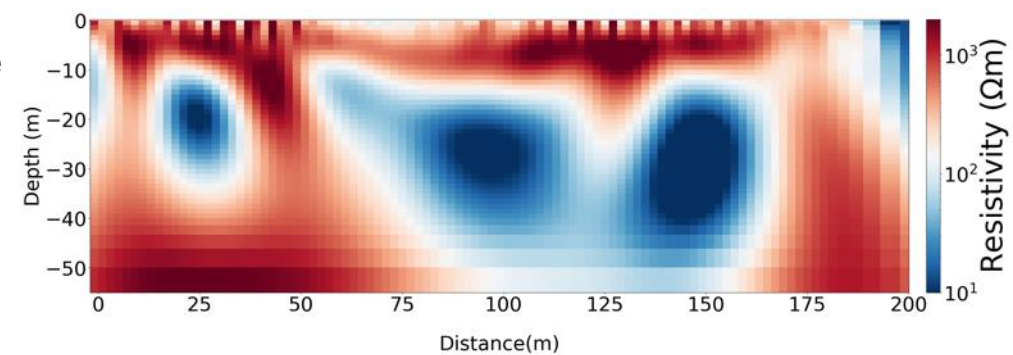
( Reference model )

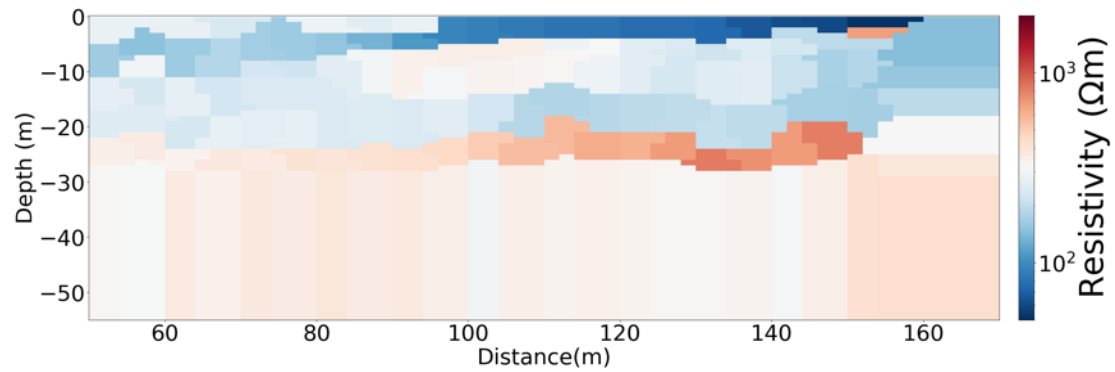
$$\rho = 10^{3*HVSR}$$

Increase

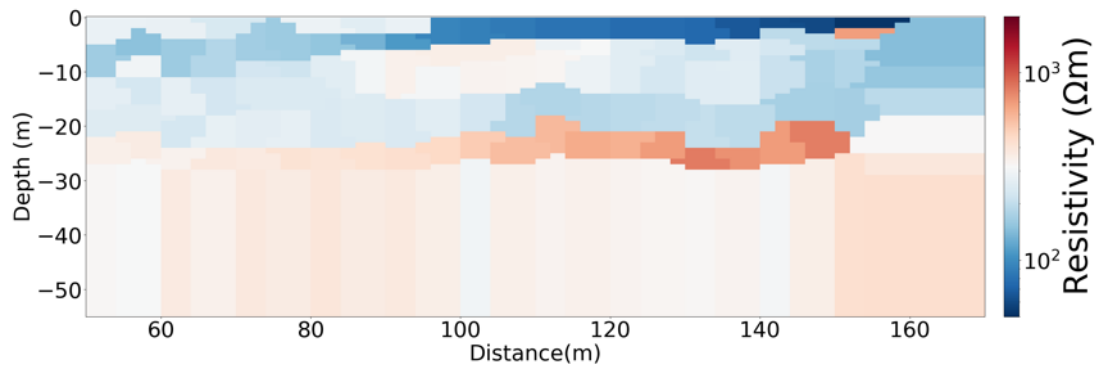
 $\alpha_s$ 

Decrease

 $\alpha_s : 1e^{-2}$  $\alpha_s : 1e^{-4}$  $\alpha_s : 1e^{-6}$ 

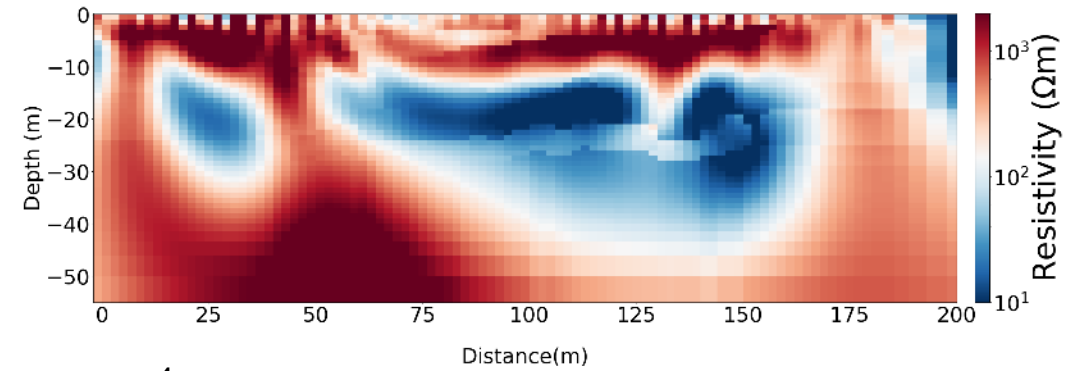
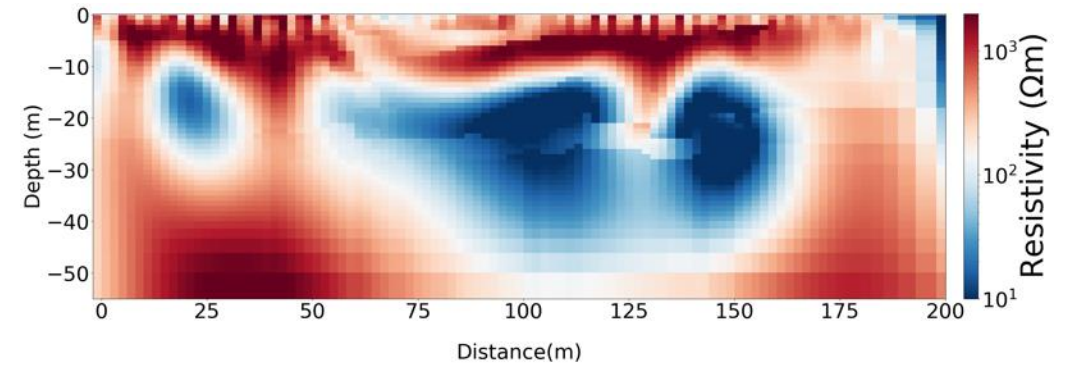
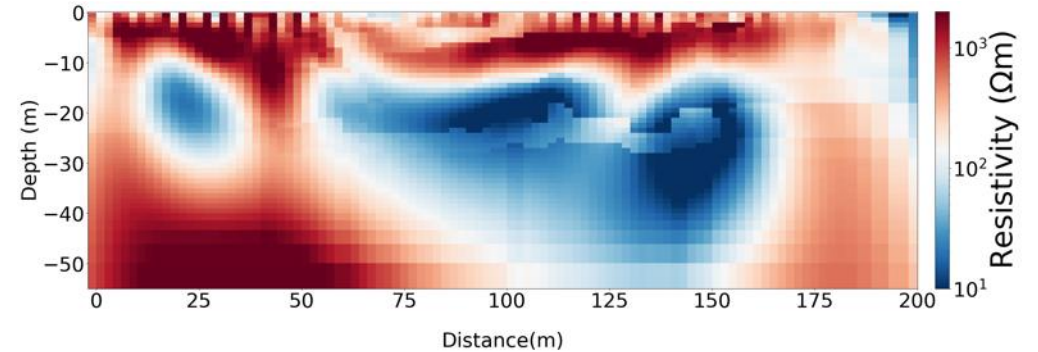


( Initial model )



( Reference model )

$$\rho = \frac{V_s + 33.289}{1.995}$$

 $\alpha_s : 1e^{-2}$ 

 $\alpha_s : 1e^{-4}$ 

 $\alpha_s : 1e^{-6}$ 




## Conclusions:

- ERT combined with ANT successfully delineated the low resistivity anomalies at 25m and 100m, 150m along the survey line
- Alternative initial and reference models from seismic can help us more thoroughly explore the model space in the electrical resistivity inversion
- Information from the velocity image can help improve the resolution at depth in ERT inversion (bottom depth of cavities)
- Uncertainties and non-uniqueness in seismic models should be considered in the future



# THANKS!

## Q & A?